

## Mechanical characterization of a self-compacting polymer concrete called isobeton

K. Boudjellal\*, M. Bouabaz and M. Belachia

*Department of Civil Engineering, LMGHU Laboratory, University 20 août 1955-Skikda, Algeria*

*(Received October 4, 2015, Revised December 31, 2015, Accepted January 4, 2016)*

**Abstract.** This paper illustrates an experimental study on a self compacting polymer concrete called isobeton made of polyurethane foam and expanded clay. Several experiments were conducted to characterize the physic-mechanical properties of the considered material. Application of the Linear Elastic Fracture Mechanics (LEFM) and determining the toughness of two isobetons based on Belgian and Italian clay, was conducted to determine the stress intensity factor  $K_{IC}$  and the rate of releasing energy  $G_{IC}$ . The material considered was tested under static and dynamic loadings for two different samples with  $10 \times 10 \times 40$  and  $10 \times 15 \times 40$  cm dimensions. The result obtained by the application of the Linear Elastic Fracture Mechanics (LEFM) shows that isobeton is optimistic and fulfilled the physic-mechanical requirement of the study.

**Keywords:** polymer concrete; polyurethane; expanded clay; linear elastic fracture mechanics; flexion

---

### 1. Introduction

Nowadays, the employment of Self Compacting Concrete (SCC) is increasing rapidly, regarding to its suitability for use in construction with excellent deformability and segregation resistance with congested reinforcement and without vibration as stated by many researchers (Khaleel *et al.* 2011, Kim *et al.* 2010, Aggarwal *et al.* 2008, Zoran *et al.* 2008, Mounanga *et al.* 2008, Aldred *et al.* 2012). Different development on the use of composite material based on polyurethane has been introduced in the literature. Amor *et al.* (2009) conducted a research on the valorization of coarse rigid polyurethane foam waste on lightweight aggregate concrete and argued in their findings that the mechanical properties of the lightweight aggregate concrete ranged between 8 and 16 MPa for the compressive strength and between 10 and 15 MPa for the dynamic modulus of elasticity, they concluded that the results consolidate the use of polyurethane for the manufacture of lightweight aggregate concrete. Jino *et al.* (2012) used fly ash as a mineral admixture in concrete, to improve its strength and durability characteristics. They suggested that fly ash can be used either as an admixture or as a partial replacement of cement. It can also be used as a partial or a total replacement of fine aggregates, or as a supplementary addition to achieve different properties of concrete. Another study carried on by (Dhiyaneshwaran *et al.* 2013, Dinakar 2008) on the durability characteristics of self compacting concrete with viscosity modifying admixture. In their investigation, the self compacting concrete was made by usual ingredients such

---

\*Corresponding author, Ph.D., E-mail: kboudjellal@yahoo.fr

Table 1 Characteristics of Belgian and Italian expanded clays

Clay type	Bulk density (kg/m <sup>3</sup> )	Absolute density (kg/m <sup>3</sup> )	Granular density (kg/m <sup>3</sup> )
Belgian clay	338	1204	435
Italian clay	261	1181	554

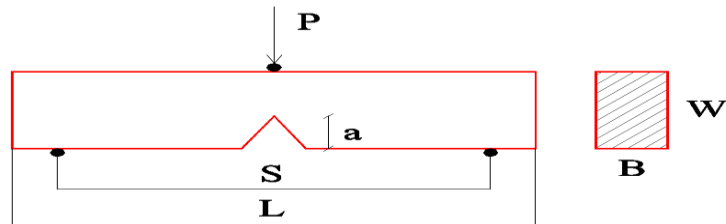


Fig. 1 Experimental setup three-point bending

as cement, aggregate, coarse aggregate, water and mineral admixture fly ash at various replacement levels.

Finally a significant work done by Yuh-Shiou *et al.* (2011) on ultra-high strength concrete describing the mechanical behavior of the material studied under repeated impact load tests. They reported that their experimental findings indicate that when a specimen is under dynamic loading, the destruction process can be considered as the result of the combined effect of strain rate hardening and damage softening.

The main objective of this contribution consists of the study of the Mechanical characterization of a self compacting polymer concrete called isobeton using the well known tests static and dynamic loadings. The result of this valuable contribution is optimistic about the application of Linear Elastic Fracture Mechanics (LEFM) to this type of composite material for use and commercialization as a building material.

## 2. Experimental study and procedure

### 2.1 Material characterization and test devices

In this study, concrete made from polyurethane and expanded clay, called isobeton, developed at Proside-Annaba, which is rich by the availability of the raw material in the region. The concrete used in this study is a mixture of polyurethane and expanded clay, prepared from Belgian and Italian clay respectively for two types as represented in Table 1.

A pendulum N 5003-0-301 shock model was used for the impact tests for metallic specimens or metal alloys in three-point bending in standard conditions of temperature and humidity. The hammer has an energy of 150 Joules with a striking aspect of knife is 4.5 cm. And a hydraulic machine with a maximum capacity of 50 KN and brand CONTROLAB Type C0010 / F, equipped with a lever arm for hand power load was used to determine the toughness of the isobeton.

### 2.2 Step one

The test pieces for the measurement of tenacity were cut from fabricated panels. Specimens

Table 2 Dimensions of the specimen

Characteristics	Parameters	Dimensions
Length	L	40 cm
Distance between supports	S	30 cm
Width	W	10 and 15 cm
Thickness	B	10 cm
Length of cut	a	/
Applied load to failure	P	/

used are prismatic side notch (PSN) cut on both isobeton panels and stressed in three-point bending. The distance (L) between the supports is 30 cm. A mapping of the experimental setup is shown in Fig. 1.

Two geometries test pieces were tested of dimensions 10×10×40 cm on panel 1 and 2, and 10×15×40 cm on panel 2.

Eight notched specimens of dimensions 10×10×40 cm with increasing lengths of notches were cut on the panel 1. For panel 2, fourteen specimens with dimensions of 10×10×40 cm and ten with dimensions of 10×15×40 cm were cut and notched. The dimensions of the specimen are presented in Table 2.

For the realization of the cuts we use a manual hacksaw. For the purpose of having very smooth cuts of funds, a very fine wood saw was used. Different lengths of cuts were performed. These lengths cuts are increasing and are chosen such that the ratio  $a/W$  remains in the following area of  $0.2 < a/W < 0.6$ , scheduled for general toughness tests. The length notch is measured using a graduated metal ruler, where  $a$  and  $W$  are respectively the length notch and the width of the specimen.

Three steps were carried out for each notch: two at the side faces and the third to the central level. The adopted value represents the arithmetic average of these three measurements. The stress intensity critical factor  $K_{IC}$  for the toughness is determined from the following Eq. (1)

$$K_{IC} = \sigma Y \sqrt{a} \quad (1)$$

where  $\sigma$  is the tensile at rupture,  $Y$  is the geometrical form factor and  $a$  is the initial notch length. The tensile is determined from the load at fracture ( $P_r$ ) and the dimensions of the test piece by the following Eq. (2)

$$\sigma = \frac{3}{2} P_r \cdot S / B \cdot W^2 \quad (2)$$

where  $S$  here is the distance between supports (30 cm),  $B$  is the specimen thickness (10 cm) and  $W$  is the width of the specimen (10 or 15 cm). The breaking load ( $P_r$ ) visually indicated on the dial of the machine corresponding to the maximum value displayed by the needle. The geometric form factor  $Y$  is given in Eq. (3) as a polynomial that varies according to the type of solicitation, and is given in three-point bending.

$$Y = 1.93 - 3.07(a/W) + 14.53(a/W)^2 - 25.11(a/W)^3 + 25.80(a/W)^4 \quad (3)$$

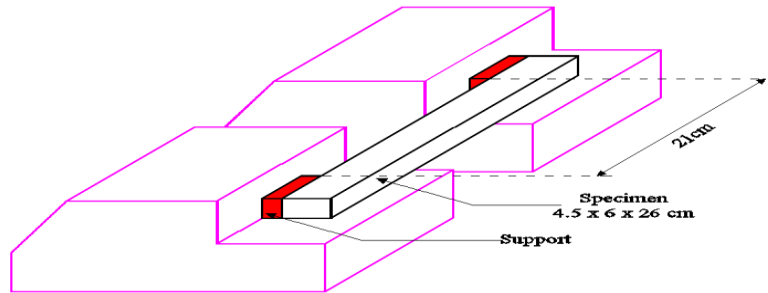


Fig. 2 Pendulum shock

### 2.3 Step two

In this part of the study, we describe the experimental procedures used according to the Fig. 2.

This test was used to characterize the material studied under dynamic loads by determining the impact strength of the material by a conventional calculation of the resilience and the release rate of the critical energy  $G_{IC}$  of the material.

Specimens of prismatic shape were used, with adopted dimensions on the imposed limitations by the support system of the experimental device. Two types of test pieces were used for this purpose; Prismatic specimens without notches 4.5×6×26 cm for measuring the resilience and 4.5×6×26 cm with notches of increasing length, for the measurement of the released rate of the critical energy  $G_{IC}$ . The distance between the supports of the device in three-point bending shock is equal to 21 cm and the resilience is determined by the following Eq. (4)

$$\sigma_{ch} = \frac{U}{BW} \quad (4)$$

where  $\sigma_{ch}$  the impact resistance,  $U$  the lost energy by the hammer after impact,  $W$  is the width of the specimen and  $B$  is the thickness. The measurement of the critical energy releasing rate  $G_{IC}$  is expressed by Eq. (5)

$$U = G_{IC} \cdot B \cdot W \cdot \phi \quad (5)$$

where  $G_{IC}$  the critical energy releasing rate, and  $\phi$  is the calibration factor given by (Williams 1973, Turner 1975).

## 3. Results and discussions

### 3.1 Test results under static load

The calculation of the stress intensity critical factor  $K_{IC}$  was done for the two panels. The values obtained are summarized in Tables 3-5.

According to Tables 3-4 and 5, the mean values obtained for  $K_{IC}$  from the two panels, seem to be significantly noisy. It is of 9.3% for panel 1, for the specimen of 10 cm width on panel 2 is in the range of 12.9% and 14.2% for panel 2 of 15cm width. The Result is summarized in Table 6.

Table 3 The  $K_{IC}$  values for different ratio ( $a/W$ ) for  $W=10$  cm width on the panel 1

N°	$a$ cm	$a$ mean cm	$a/W$	$P_r$ KN	$\sigma$ MPa	$K_{IC}$ MPa m <sup>1/2</sup>	$K_{IC}$ mean MPa m <sup>1/2</sup>	$E.T$ MPa m <sup>1/2</sup>	C.V %
1	4.75, 4.70, 4.80	4.75	0.48	0.8	0.036	0.19			
2	4.70, 4.60, 4.80	4.70	0.47	1.0	0.045	0.23			
3	4.10, 4.20, 4.10	4.13	0.41	1.2	0.054	0.23			
4	3.80, 3.60, 3.70	3.70	0.37	1.2	0.054	0.21	0.21	0.02	9.30
5	2.70, 2.70, 2.80	2.73	0.27	1.8	0.081	0.24			
6	2.70, 2.50, 2.70	2.63	0.26	1.6	0.072	0.21			
7	2.00, 1.80, 1.90	1.90	0.19	1.8	0.081	0.19			
8	2.00, 1.75, 1.80	1.85	0.19	1.8	0.081	0.19			

Table 4 The  $K_{IC}$  values for different ratio ( $a/W$ ) for  $W=10$  cm width on the panel 2

N°	$a$ cm	$a$ mean cm	$a/W$	$P_r$ KN	$\sigma$ MPa	$K_{IC}$ MPa m <sup>1/2</sup>	$K_{IC}$ mean MPa m <sup>1/2</sup>	$E.T$ MPa m <sup>1/2</sup>	C.V %
1	2.10, 2.30, 2.20	2.20	0.22	1.70	0.077	0.20			
2	2.20, 2.30, 2.20	2.23	0.22	1.30	0.059	0.15			
3	2.90, 3.10, 3.20	3.06	0.31	1.20	0.054	0.18			
4	3.00, 2.80, 3.00	2.93	0.29	1.20	0.054	0.17			
5	4.20, 4.10, 4.00	4.10	0.41	0.80	0.036	0.15			
6	3.90, 3.80, 3.90	3.87	0.39	1.10	0.050	0.20			
7	5.00, 5.00, 5.10	5.03	0.50	0.80	0.036	0.20	0.18	0.02	12.9
8	5.20, 5.30, 5.30	5.27	0.53	0.60	0.027	0.17			
9	5.20, 5.30, 5.30	5.23	0.52	0.60	0.027	0.16			
10	5.70, 5.70, 5.70	5.70	0.57	0.70	0.032	0.22			
11	2.00, 1.80, 2.00	1.93	0.19	1.72	0.077	0.19			
12	2.00, 2.00, 2.10	2.03	0.20	1.24	0.056	0.14			
13	3.50, 3.40, 3.30	3.40	0.34	1.10	0.050	0.18			
14	3.60, 3.60, 3.60	3.60	0.36	1.20	0.054	0.20			

Table 5 The  $K_{IC}$  values for different ratio ( $a/W$ ) for  $W=15$  cm width on the panel 2

N°	$a$ cm	$a$ mean cm	$a/W$	$P_r$ KN	$\sigma$ MPa	$K_{IC}$ MPa m <sup>1/2</sup>	$K_{IC}$ mean MPa m <sup>1/2</sup>	$E.T$ MPa m <sup>1/2</sup>	C.V %
1	3.10, 2.90, 3.00	3.00	0.20	0.20	0.054	0.16			
2	3.10, 2.90, 3.00	3.00	0.20	0.20	0.068	0.20			
3	4.40, 4.30, 4.40	4.36	0.29	0.29	0.048	0.18			
4	4.30, 4.00, 4.10	4.13	0.28	0.28	0.052	0.19			
5	6.00, 6.10, 6.00	6.03	0.40	0.40	0.040	0.20	0.21	0.03	14.2
6	6.20, 6.00, 6.10	6.10	0.41	0.41	0.040	0.21			
7	7.20, 7.10, 7.10	7.13	0.48	0.48	0.036	0.23			
8	7.10, 7.10, 7.00	7.06	0.47	0.47	0.034	0.21			
9	8.50, 8.50, 8.40	8.46	0.57	0.57	0.028	0.24			
10	8.70, 8.80, 8.90	8.80	0.59	0.59	0.030	0.28			

Table 6 Obtained values for different ratios

Panel	Maximum value	Minimum value	$K_{IC}$ mean MPa m <sup>1/2</sup>	$E.T$ MPa m <sup>1/2</sup>	$C.V$ %
W=10 cm width on the panel 1	0.24	0.19	0.21	0.020	09.30
W=10 cm width on the panel 2	0.22	0.15	0.18	0.020	12.90
W=15 cm width on the panel 2	0.28	0.16	0.21	0.030	14.20

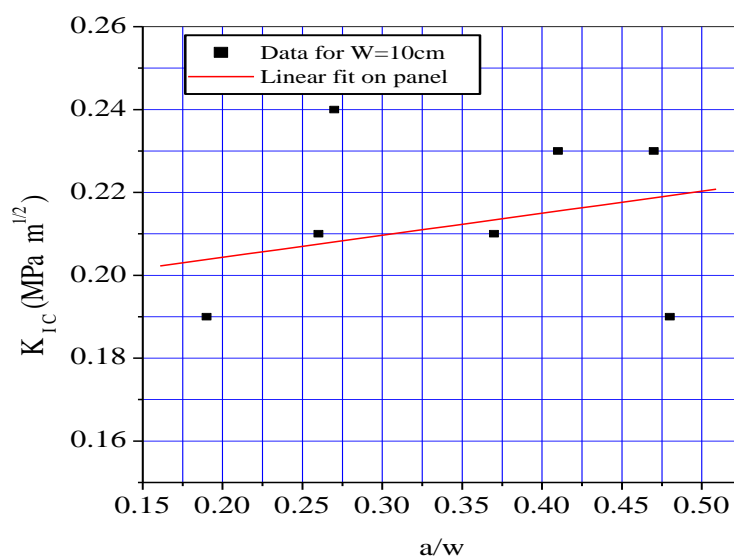


Fig. 3 Variation of the stress intensity factor versus the ratio for 10 cm width on panel 1

### 3.1.1 Effect of the ratio ( $a/W$ ) on $K_{IC}$

Figs. 3-5 show the dispersion of the experimental points with respect to the mean line as can be observed. This dispersion is due in large part to the heterogeneity of the material on the way to cracking. The break does not occur often in the extension of the initial cut. Indeed, cracking always follows the path of least resistance. Thus, under the influence of loading a pre-existing crack can progress through the foam-aggregate interfaces. There are often, sudden changes of direction of the crack during its propagation and bifurcations which gives a tortuous nature to cracking. The variation of the stress intensity factor  $K_{IC}$  calculated according to the ratio,  $a/W$  is presented graphically in Figs. 3-5.

This phenomenon suggests that, the crack propagation differs from one specimen to another which consequently induces strong dispersion observed in the  $K_{IC}$  measured values. However, the heterogeneity of the isobeton cannot be alone the main origin of this high dispersion. The uniformity and the radius of the bottom of notch as they were executed with a manual hacksaw and checked visually, certainly differ from one notch to another. This difference also contributes to the increase of the dispersion in the measurement of  $K_{IC}$ . However, this dispersion is of the same order of magnitude as that normally seen on ordinary concrete or on reinforced concrete of short metal fibers. Closeness of  $K_{IC}$  values of the two panels were predictable because of the very similar physic-mechanical properties of expanded clay used in both isobetons. Moreover, the  $K_{IC}$  values of the two panels seem little affected by the variation of the specimen width.

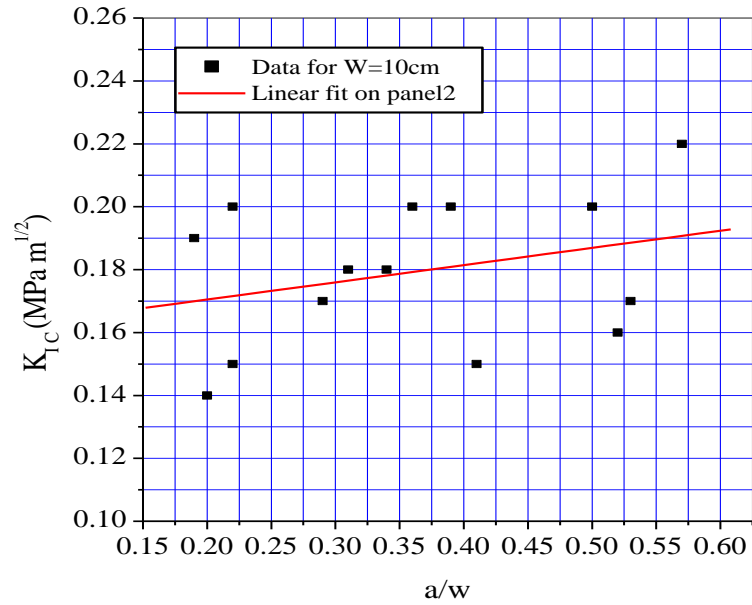


Fig. 4 Variation of the stress intensity factor versus the ratio for 10 cm width on panel 2

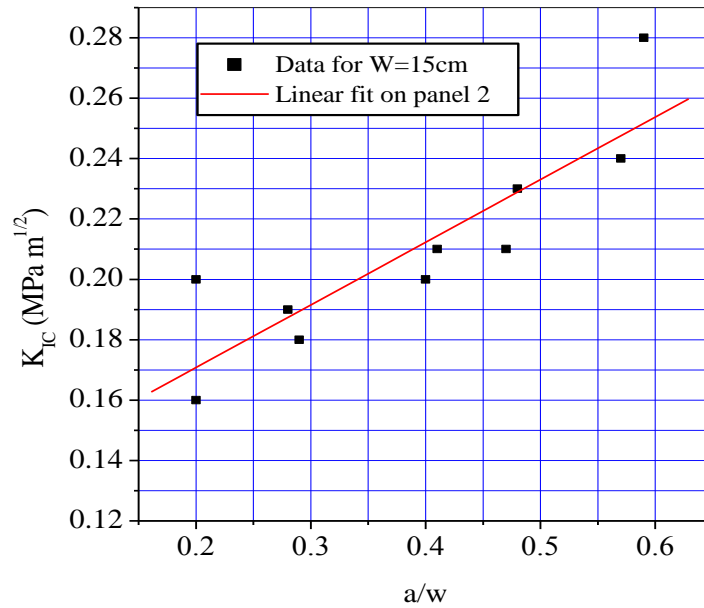


Fig. 5 Variation of the stress intensity factor versus the ratio for 15 cm width on panel 2

### 3.2 Test results under dynamic load

For the test of resilience performed on six test pieces of the panel 1, the result is summarized in Table 7, and the test result of impact toughness test pieces for different lengths isobeton with notches cut in the panels 1 and 2 is summarized in Tables 8-9.

Table 7 Measured values for the resilience on Panel 1

N°	$U$ (Joule)	$\sigma_{ch}$ (kJ/m <sup>2</sup> )	$\sigma_{ch\ mean}$ (kJ/m <sup>2</sup> )	$E.T.$ (kJ/m <sup>2</sup> )	$C.V.$ (%)
1	45.00	16.66			
2	82.50	30.55			
3	60.00	22.22	23.74	7.098	29.89
4	43.50	16.11			
5	96.00	35.55			
6	57.60	21.33			

Table 8 Measured and calculated values of  $U$  and  $BW\phi$  for different specimens cut on Panel 1

N°	$a$ (cm)	$a$ Mean (cm)	$a/W$	$\phi$	$BW\phi$ 10 <sup>-4</sup> (m <sup>2</sup> )	$U_{IC}$ 10 <sup>-3</sup> (kJ)
1	1.20, 1.20	1.20	0.200	0.427	11.529	57.6
2	1.20, 1.25	1.23	0.205	0.421	11.367	100.5
3	1.20, 1.20	1.20	0.200	0.427	11.529	80.4
4	1.60, 1.80	1.70	0.283	0.343	9.361	93.0
5	1.60, 1.60	1.60	0.267	0.357	9.639	81.6
6	1.60, 1.60	1.60	0.267	0.357	9.639	96.0
7	2.00, 2.00	2.00	0.310	0.310	8.370	100.0
8	2.00, 2.00	2.00	0.310	0.310	8.370	91.2
9	1.90, 1.95	1.93	0.317	0.317	8.559	82.5
10	2.40, 2.40	2.40	0.273	0.273	7.371	74.4
11	2.30, 2.30	2.30	0.282	0.282	7.614	100.2
12	2.30, 2.20	2.25	0.286	0.286	7.722	69.6
13	2.50, 2.45	2.47	0.267	0.264	7.209	60.9
14	2.50, 2.50	2.50	0.264	0.267	7.128	64.8
15	2.40, 2.45	2.42	0.271	0.271	7.317	66.0
16	2.60, 2.60	2.60	0.257	0.257	6.939	30.6
17	2.55, 2.60	2.57	0.257	0.259	6.993	43.8
18	2.65, 2.70	2.67	0.251	0.251	6.777	55.2
19	3.00, 3.00	3.00	0.225	0.225	6.075	84.0
20	2.95, 2.95	2.95	0.224	0.224	6.048	51.3
21	2.95, 3.00	2.97	0.226	0.226	6.102	69.6
22	3.15, 3.20	3.17	0.213	0.213	5.751	107.1
23	3.20, 3.25	2.23	0.209	0.209	5.643	68.1
24	3.30, 3.25	3.28	0.205	0.205	5.535	110.4

As shown in tables 8-9, the measured values of the energy absorbed by the test pieces of the two panels are characterized by a high dispersion as in the case of non-notched specimens. It is 27% for the panel 1 and 38.4% for the panel 2. This high dispersion characteristic is the heterogeneity of the isobeton well as the impact test itself.

Table 9 Measured and calculated values of  $U$  and  $BW\emptyset$  for different specimens cut on Panel 2

N°	$a$ (cm)	$a$ mean (cm)	$a/w$	$\emptyset$	$BW\emptyset$ $10^{-4}(m^2)$	$U_{IC}$ $10^{-3}$ (kJ)
1	1.50, 1.50	1.50	0.250	0.372	10.044	51.00
2	1.30, 1.30	1.30	0.220	0.402	10.854	88.80
3	1.30, 1.30	1.30	0.220	0.402	10.854	75.00
4	1.30, 1.30	1.30	0.220	0.402	10.354	46.50
5	1.70, 1.70	1.70	0.280	0.345	09.099	96.90
6	1.70, 1.80	1.75	0.290	0.337	08.586	55.80
7	1.90, 1.90	1.90	0.320	0.318	08.586	46.20
8	2.00, 2.00	2.00	0.320	0.318	08.586	33.00
9	1.90, 1.95	1.93	0.360	0.293	07.911	50.40
10	2.30, 2.30	2.30	0.380	0.283	07.641	36.90
11	2.70, 2.70	2.70	0.450	0.249	07.723	48.20
12	2.50, 2.40	2.45	0.410	0.268	07.236	33.60
13	2.90, 3.20	3.10	0.510	0.221	05.967	78.00
14	3.50, 3.50	3.50	0.580	0.191	05.157	98.00
15	3.10, 3.30	3.20	0.530	0.213	05.751	37.80
16	2.80, 3.00	2.90	0.480	0.235	06.345	28.80
17	3.10, 3.31	3.20	0.530	0.213	05.751	74.10
18	3.10, 3.10	3.10	0.520	0.217	05.859	66.00

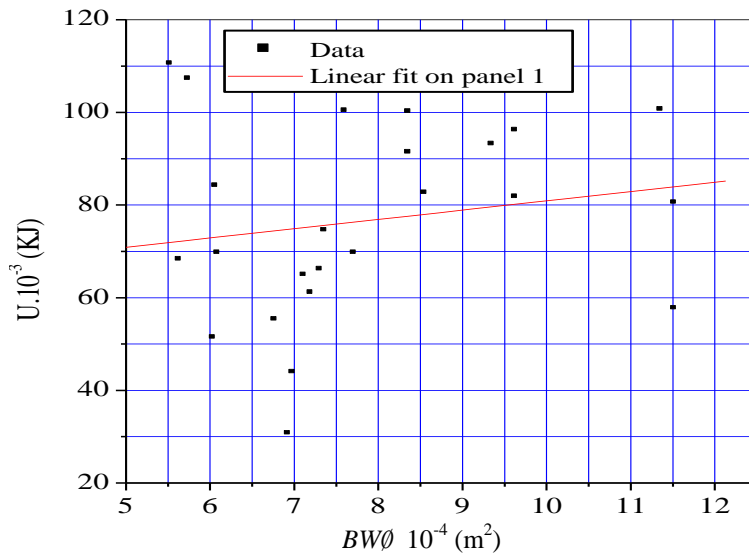


Fig. 6 Variation of  $U$  as a function of  $BW\emptyset$  for the panel 1

### 3.2.1 Variation of the breaking energy $U$ according to $BW\emptyset$

The result obtained for the panels 1 and 2 shows the variations of the breaking energy  $U$  according to  $BW\emptyset$ . Theoretically this variation should be linear and the slope of the line represents

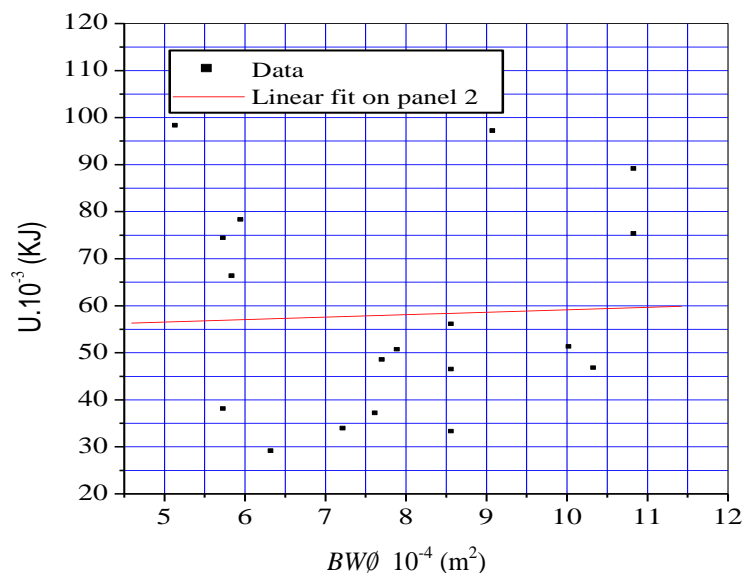


Fig. 7 Variation of  $U$  as a function of  $BW\emptyset$  for the panel 2

the energy release rate  $G_{IC}$  as presented in Figs. 6-7.

The experimental points are plotted around the mean line. The break is not often performed in line with the initial cut. Indeed, cracking always follows the path of least resistance. Thus, under the influence of loading a pre-existing crack can progress through the foam-aggregate between the interfaces which are weak areas. There is often a sudden change of direction of the crack during its propagation and a bifurcation giving a tortuous crack this phenomenon suggests that the propagation of the crack to specimen differs from other which indicates a high dispersion as shown in Figs. 6-7.

The experimental points as obtained are characterized by dispersion around the regression line. Indeed, the correlation coefficients are equal to 0.21 and 0.14 respectively for the corresponding lines in the panel 1 and the panel 2. The  $G_{IC}$  values represent the regression straight slopes on the set of points measured for the two panels and which are respectively;  $12.87 \text{ kJ/m}^2$  on panel 1 and  $9.17 \text{ kJ/m}^2$  for panel 2.

The calibration factor  $\emptyset$  used to determine the  $G_{IC}$  is tabulated for a set of polymers with the intermediate values determined by interpolation according to (Williams 1973, Turner 1975). For the tenacity at static regime, the values obtained under dynamic loading are very close, with a slight difference observed on the values of the two panels is only due to the heterogeneity of the isobeton and the dispersion of the impact test.

#### 4. Conclusions

The result of this study conducted to the following conclusions:

- The intensity factor of the critical constraints  $K_{IC}$ , determined by the principles of Linear Elastic Fracture Mechanics is characterized by a high dispersion. This dispersion was observed on both panels.

- The intensity factor of the critical constraints  $K_{IC}$ , of the isobeton based on Belgian expanded clay is identical to that isobeton based on Italian clay.
- The  $K_{IC}$  values obtained for the two isobetons are comparable to those obtained on lightweight concrete based on similar materials (Pozolan).
- The considered isobeton has acceptable impact strength.
- The values of the rate of energy restitution  $G_{IC}$  obtained are very low compared to those obtained on ordinary concrete. However, considering to the poor mechanical performance of the isobeton compared to those of an ordinary hydraulic concrete, the obtained  $G_{IC}$  values are reasonable and acceptable.
- The damage mechanism of rupture the most dominant is probably due to the loosening and abruption of the matrix aggregates. Therefore, the creation of new surfaces of rupture does not require a large amount of energy in the case of this material, because of the low adhesion between the grains and the matrix. This explains the low value of the rupture energy  $G_{IC}$  of this type of composite material.
- The results are optimistic and fulfilled the requirement about the application of the Linear Elastic Fracture Mechanics (LEFM) to this type of composite material.

## References

- Aggarwal, P., Siddique, R., Aggarwal, Y. and Gupta, S.M. (2008), "Self-compacting concrete-procedure for mix design", *Leon. Elec. J. Pract. Tech.*, **12**, 15-24.
- Aldred, J. and John, D. (2012), "Is geopolymer concrete a suitable alternative to traditional concrete", *37th Conference on Our World in Concrete & Structures*, Singapore.
- Ben Fraj, A., Kismi, M. and Mounanga, P. (2009), "Valorisation of coarse rigid polyurethane foam waste in lightweight aggregate concrete", *Constr. Build. Mater.*, **24**(6), 1069-1077.
- Dhiyaneshwaran, S., Ramanathan, P., Baskar, I. and Venkatasubramani, R. (2013), "Study on durability characteristics of self compacting concrete with fly ash", *Jordan J. Civil Eng.*, **7**(3), 342-353.
- Dinakar, P., Babu, K.G. and Santhanam, M. (2008), "Durability properties of high volume fly ash self compacting concretes", *Cement Concrete Compos.*, **30**(10), 880-886.
- Jino, J., Maya, T.M. and Meenambal, T. (2012), "Mathematical modelling for durability characteristics of fly ash concrete", *Int. J. Eng. Sci. Tech.*, **4**(1), 353-361
- Khaleel, O.R., Al-Mishhadani, S.A. and Razak, H.A. (2011), "The effect of coarse aggregate on fresh and hardened properties of self-compacting concrete (SCC)", *Procedia Eng.*, **14**, 805-813.
- Kim, Y.J., Choi, Y.W. and Lachemi, M. (2010), "Characteristics of self-consolidating concrete using two types of lightweight coarse aggregates", *Constr. Build. Mater.*, **24**, 11-16.
- Mounanga, P.W.G., Poullain, P. and Turcry, P. (2008), "Proportioning and characterization of lightweight concrete mixtures made with rigid polyurethane foam wastes", *Cement Concrete Compos.*, **30**, 806-814.
- Turner, C.E. (1973), "Fracture toughness and specific fracture energy: a re-analysis of results", *J. Mater. Sci. Eng.*, **11**(5), 241-304.
- Williams, J.G. and Platini, E. (1975), "The determination of the fracture parameters for polymers in impact", *Polym. Eng. Sci.*, **15**(6), 470-477.
- Yuh-Shiou, T. and Lau-The, W. (2011), "Elucidating the mechanical behaviour of ultra-high-strength concrete under repeated impact loading", *Struct. Eng. Mech.*, **37**(1), 1-15.
- Zoran, G., Despotović, I. and Gordana, T. C. (2008), "Properties of self compacting concrete with different types of additives", *Facta Univ. Ser. Arch. Civil Eng.*, **6**(2), 173- 177.